BF_2-Complexes of Carbazole–Benzimidazole Conjugates: Synthesis, Structures, and Spectroscopic Properties

Ranjan Dutta,[†] Dikhi Firmansyah,[†] Jaeduk Yoo,[†] Ravi Kumar,[†] Endale Mulugeta,[†] Hongil Jo,[‡] Kang Min Ok,[‡] and Chang-Hee Lee[†,*]

[†]*Department of Chemistry, Kangwon National University, Chuncheon 24341, Korea.*
**E-mail: chhlee@kangwon.ac.kr*
[‡]*Department of Chemistry, Chung-Ang University, Seoul 06974, Korea*
Received July 7, 2017, Accepted August 2, 2017, Published online August 30, 2017

A series of carbazole–benzimidazole conjugates and corresponding BF_2-complexes (BODIPYs) are synthesized and characterized. Carbazole–benzimidazole conjugates are synthesized by the condensation of 1-formyl carbazole and phenylene diamines in good yields. Various substituents are introduced into the benzimidazole moiety and subsequent reaction with BF_3•Et_2O afforded the BF_2-complexes in moderate to good yield. The structural and photophysical properties of the synthesized fluorophores are investigated with various spectroscopic techniques such as UV/Vis and fluorescence spectroscopy, cyclic voltammetry and X-ray crystallography.

Keywords: Fluorescence dyes, BODIPY, Carbazole, Stokes shift, Benzimidazole

Introduction

Borron dipyrromethenes (BODIPYs) have emerged as a prevalent functional dyes due to their application in biomolecule markers, fluorescent switches, photodynamic therapy, organic solar cells, chemosensors, laser dyes, and fluorescence labeling of surface.[1–13] Moreover, development of new synthetic strategies for their functionalization enables their attachment to biological substrate and also to tune their optical properties. Such new strategies include halogenation and subsequent aromatic nucleophilic substitution of the dipyrrin core, cross-coupling reaction or nucleophilic substitution reaction at the boron center by alkynes or alchohols.[14–18] The most important challenges in recent BODIPY chemistry are directed towards the development of dyes with longer-wavelength absorption and emission profiles, and the preparation of dyes with additional functional groups.[19–21]

Carbazole–benzimidazole conjugates are known for biological activities such as sequence specific DNA binding.[22] Such bipolar hybrid molecules also found application in phosphorescent material development.[23,24] Maeda *et al.* have shown the incorporation of carbazole units to porphyrinoids and BODIPY frameworks generated interesting photophysical properties.[25–27] A recent report on four-coordinate organoboron complexes derived from indole-azaheteroaryl ligands showed wide range of emission from blue to orange.[28] However, small Stokes shifts (<15 nm) are one of the main drawbacks for the application of BODIPY dyes in molecular imaging due to the self-absorption effect resulting in less intensive emission.[29] Carbazole-based BODIPYs exhibit large Stokes shifts and moderate to high fluorescence quantum yield as reported by Maeda *et al.* in a recent study.[27] With these regards, we designed novel BODIPY analogs containing additional nitrogen on the core part of the molecule. The design was based on the conjugation of the two fluorophores such as carbazole and benzimidazole, whereas the corresponding boron complexes can be constructed easily. Thus, benzimidazole, N-alkyl/aryl benzimidazole and substituted benzimidazole are introduced to the 1-position of carbazole and the respective BF_2-complexes are synthesized. The newly synthesized BODIPY-complexes exhibited relatively higher quantum yield while maintaining large Stokes shifts compared to the normal BODIPY.

Experimental

Materials and Methods. All commercially available compounds were used as received. Transformation- and oxygen-sensitive compounds were performed under a nitrogen atmosphere. The reaction progress was monitored by thin layer chromatography (TLC) on glass sheets that were coated with silica gel 60 F254 (MN), with detection by a UV lamp. Product purification was performed by column chromatography on silica (230–400 mesh, MN). The identity and purity of the prepared compounds were confirmed by ^{1}H NMR and ^{13}C NMR spectroscopy (Bruker 400/300 MHz, Billerica, MA, USA). Mass spectra were recorded on Voyager DE-STR MALDI-TOF and JEOL JMS-700 GC (Tokyo, Japan) mass spectrometer. 1-Formylcarbazole (**4**) is synthesized following a modified literature procedure.[30]

General Synthesis for 6a, 6b, 6c, and 9. 1-Formylcarbazole (1 equiv) **4**, 1,2-phenylene diamine (1.2 equiv), *p*-toluenesulfonic acid (10%) in 10 mL of EtOH were refluxed for 24 h under argon atmosphere. The solvent was removed, 10 mL of water was added, and the

mixture was extracted with DCM (3 × 10 mL). The combined organic layers were dried on $MgSO_4$, filtered, and concentrated *in vacuo*. The residue was purified by chromatography on silica gel using Hexane/DCM as eluents to give the desired product.

Compound **6a:** Yellow solid (yield 64%), ^{1}H NMR (DMSO-d_6, 300 MHz) 13.12 (br, s, 1H), 11.64 (br, s, 1H), 8.28 (d, J = 8 Hz, 1H), 8.20 (d, J = 8 Hz, 2H), 8.18 (d, J = 8 Hz, 1H), 7.72 (s, 2H), 7.47 (t, J = 8 Hz, 1H), 7.44 (d, J = 8 Hz, 1H), 7.39 (t, J = 8 Hz, 2H), 7.28 (t, J = 8 Hz, 1H).

^{13}C NMR (DMSO-d_6, 100 MHz) 151.05, 139.9, 137.14, 126.06, 123.73, 122.85, 122.0, 121.93, 120.24, 119.19, 118.59, 112.28, 112.2 ppm. HRMS calculated for $C_{19}H_{13}N_3$ exact mass: 283.1109; found: 283.1107.

Compound **6b**: Colorless solid (yield 72%) ^{1}H NMR (300 MHz, DMSO-d_6): δ (ppm) 11.32 (s, 1H), 8.34 (d, J = 7.2 Hz, 1 H), 8.22 (d, J = 7.8 Hz, 1 H), 7.81 (t, J = 7.1 Hz, 2 H), 7.71(d, J = 7.4 Hz, 1H), 7.65 (d, J = 8.1 Hz, 1 H), 7.43 (t, J = 7.7 Hz, 1 H), 7.37 (t, J = 7.6 Hz, 2 H), 7.33 (td, J = 7.1, 1.1 Hz, 1 H), 7.2 (t, J = 7.6 Hz, 2 H), 3.92 (s, 1H).

^{13}C NMR (acetone-d_6, 100 MHz) 152.29, 143.9, 141.09, 139.93, 137.62, 127.0, 126.14, 125.10, 123.75, 123.48, 122.94, 122.50, 121.10, 120.21, 120.03, 119.33, 113.82, 112.44, 110.97, 32.84 ppm. HRMS calculated for $C_{20}H_{15}N_3$ exact mass: 297.1266; found: 297.1264.

Compound **6c**: Colorless solid (yield 56%) ^{1}H NMR (DMSO-d_6, 400 MHz) 11.47 (s, 1H), 8.18 (t, J = 7.2 Hz, 2H), 7.95 (d, J = 7.8 Hz, 1H), 7.73 (d, J = 8.1 Hz, 1H), 7.52–7.59 (m, 3H), 7.48–7.50 (m, 2H), 7.31–7.45 (m, 3H), 7.19–7.24 (m, 2H), 7.11 (dd, 1H), 7.03 (t, J = 7.6 Hz, 1H).

^{13}C NMR (DMSO-d_6, 100 MHz) 150.54, 142.92, 140.33, 138.61, 137.16, 137.0, 130.44, 129.32, 127.86, 126.43, 125.94, 123.91, 123.82, 123.11, 122.42, 122.09, 120.60, 119.74, 119.48, 118.20, 112.68, 112.25, 100.74 ppm. HRMS calculated for $C_{25}H_{17}N_3$ exact mass: 359.1422; found: 359.1423.

Compound **9**: Light yellow solid (yield 68%) ^{1}H NMR (DMSO-d_6, 300 MHz) δ (ppm) 8.31 (d, J = 8 Hz, 1H), 8.21 (d, J = 8 Hz, 1H), 8.15 (d, J = 8 Hz, 1H), 7.79 (d, J = 8 Hz, 1H, broad signals corresponding to two more protons possibly due to tautomerization), 7.50 (t, J = 8 Hz, 1H), 7.42 (d, J = 8 Hz, 1H), 7.39 (t, J = 8 Hz, 1H), 7.28 (t, J = 8 Hz, 1H).

^{13}C NMR (DMSO-d_6, 100 MHz): 152.27, 139.93, 137.18, 126.14, 125.05, 123.84, 123.10, 122.35, 121.96, 120.26, 119.27, 118.60, 112.27, 111.70 ppm. HRMS calculated for $C_{19}H_{12}N_3Br$ exact mass: 361.0215; found: 361.0218.

General synthesis for BODIPYs. Respective benzimidazole-carbazole derivative (1 equiv) was dissolved in dry DCM and NEt_3 (10 equiv) was added. After stirring for 5 min, $BF_3{\cdot}OEt_2$ (20 equiv) was added to the solution. Then the mixture was stirred for 16 h at room temperature. The solvent was removed, 30 mL of water was added, and the mixture was extracted with EtOAc (3 × 10 mL). The combined organic layers were dried on Na_2SO_4, filtered, and concentrated in vacuo. The residue was purified by column chromatography on silica gel using hexane/ethyl acetate as eluent.

Compound **7a**: Yellow solid (yield 38%), ^{1}H NMR (DMSO-d_6, 400 MHz) δ (ppm) 14.95 (br, s, 1H), 8.47 (d, J = 6.8 Hz, 1H), 8.32 (d, J = 8 Hz, 1H), 8.27 (d, J = 7.6 Hz, 1H), 8.05–8.0 (m, 1H), 7.90–7.85 (m, 1H), 7.81 (d, J = 8 Hz, 1H), 7.61–7.55 (m, 2H), 7.53 (t, 8 Hz, 1H), 7.45 (t, J = 7.6 Hz, 1H), 7.29 (t, J = 6.8 Hz, 1H).

^{13}C NMR (DMSO-d_6, 100 MHz) 147.76, 142.74, 140.53, 133.54, 132.74, 126.94, 125.91, 125.73, 125.32, 124.13, 124.0, 121.99, 121.52, 120.29, 119.17, 115.87, 113.66, 104.92 ppm. HRMS exact mass calculated for $C_{19}H_{12}N_3BF_2$: 331.1092; found: 331.1938 $[M]^+$, 312.1929 $[M\text{-}F]^+$.

Compound **7b**: Yellow solid (yield 49%), ^{1}H NMR (DMSO-d_6, 400 MHz) δ (ppm) 8.52 (d, J = 7.6 Hz, 1H), 8.49 (d, J = 8 Hz, 1H), 8.28 (d, J = 8 Hz, 1H), 8.13–8.02 (m, 2H), 7.81 (d, J = 8 Hz, 1H), 7.65–7.59 (m, 2H), 7.54 (t, J = 8 Hz, 1H), 7.47 (t, 8 Hz, 1H), 7.32 (t, 8 Hz, 1H), 4.47 (s, 3H).

^{13}C NMR (DMSO-d_6, 100 MHz) δ 147.45, 143.13, 141.48, 135.68, 133.17, 127.67, 126.47, 124.90, 124.84, 122.10, 121.15, 119.89, 116.71, 114.36, 113.20, 106.30, 34.39 ppm, HRMS calculated for $C_{20}H_{14}BF_2N_3$ exact mass: 345.1249; found: 345.1246.

Compound **7c**: Yellow solid (yield 82%) ^{1}H NMR (DMSO-d_6, 400 MHz) δ (ppm) 8.39 (d, J = 7.5 Hz, 1H), 8.26 (d, J = 8 Hz, 1H), 8.16 (d, J = 8 Hz, 1H), 8.00–7.98 (m, 2H), 7.90–7.83 (m, 4H), 7.67 (td, $J1$ = 0.7 Hz, $J2$ = 8 Hz, 1H), 7.56 (td, $J1$ = 8 Hz, $J2$ = 0.7 Hz, 1H), 7.32 (t, J = 7.5 Hz, 1H), 7.23 (d, J = 7.5 Hz, 1H), 7.07 (t, J = 8 Hz, 1H), 6.80 (d, J = 8 Hz, 1H).

^{13}C NMR (DMSO-d_6, 100 MHz) δ 147.32, 143.29, 141.86, 136.80, 135.39, 133.32, 132.71, 132.30, 129.44, 127.85, 127.20, 126.87, 126.66, 125.17, 124.82, 122.94, 122.21, 121.26, 119.43, 116.92, 114.39, 112. 85, 105.51 ppm. HRMS calculated for $C_{25}H_{16}BF_2N_3$ exact mass: 407.1405; found: 407.1403.

Compound **10a**: Yellow solid (yield 25%) ^{1}H NMR (DMSO-d_6, 400 MHz) δ (ppm) 15.13 (br, s, 1H), 8.48 (dd, $J1$ = 0.8 Hz, $J2$ = 7.6 Hz, 1H), 8.32 (dd, $J1$ = 0.8 Hz, $J2$ = 8 Hz, 1H), 8.26 (d, J = 7.6 Hz, 1H), 8.08 (d, J = 1.6 Hz, 1H), 7.94 (d, J = 8.8 Hz, 1H), 7.78 (d, J = 8 Hz, 1H) 7.73 (dd, $J1$ = 1,6 Hz, $J2$ = 8.8 Hz, 1H), 7.54 (td, $J1$ = 0.8 Hz, $J2$ = 8.4 1H) 7.45 (t, J = 7.6 Hz, 1H), 7.31 (td, $J1$ = 0.8 Hz, $J2$ = 8 Hz, 1H).

^{13}C NMR (DMSO-d_6, 100 MHz) δ 148.81, 142.69, 140.64, 134.34, 132.86, 128.29, 126.99, 126.0, 124.12, 124.06, 122.26, 121.54, 120.37, 119.22, 117.96, 117.42, 116.39, 113.62, 104.80 ppm. Molecular weight calculated for $C_{19}H_{11}N_3BF_2Br$: 410.02; found: 391.0 $(M\text{-}F)^+$.

Compound **10b**: Yellow solid (yield 24%) ^{1}H NMR (DMSO-d_6, 400 MHz) δ (ppm) 15.14 (br, s, 1H), 8.47 (d,

J = 7.6 Hz, 1H), 8.29 (d, J = 7.6 Hz, 1H), 8.26 (d, J = 8 Hz, 1H), 8.09 (s, 1H), 7.84 (d, J = 8.8 Hz, 1H), 7.78 (d, J = 8.4 Hz, 1H), 7.72 (dd, $J1$ = 1.2 Hz, $J2$ = 8.2 Hz, 1H), 7.54 (td, $J1$ = 1.2 Hz, $J2$ = 7.4 Hz, 1H) 7.45 (t, J = 8, 1H), 7.31 (td, $J1$ = 0.8 Hz, $J2$ = 7.4 Hz, 1H).

^{13}C NMR (DMSO-d_6, 100 MHz) δ 148.87, 142.67, 140.64, 134.78, 132.33, 128.64, 127.03, 126.06, 124.11, 122.25, 121.55, 120.40, 119.28, 117.99, 117.20, 115.73, 113.61, 104.74 ppm. Molecular weight calculated for $C_{19}H_{11}N_3BF_2Br$: 410.02; found: 391.0 $(M\text{-}F)^+$.

Photophysics. CH_2Cl_2 was HPLC grade (Aldrich, Seoul, Korea). Absorption spectra were recorded with a Varian CARY 100 Conc spectrophotometer (Sydney, Australia) and the emission spectra were recorded using Scinco FS-2 fluorescence spectrophotometer (Seoul, Korea). Luminescence quantum yields of the samples, Φ_s, were evaluated against a standard with known emission quantum yield, Φ_r, by comparing areas under the corrected luminescence spectra using the equation: $\Phi_s/\Phi_r = A_r n^2_s$ (area)$_s$/ $A_s n^2_r$ (area)$_r$, where A is the absorbance, n is the refractive index of the solvent employed and s and r stand for sample and reference, respectively. The standard used was air-equilibrated quinine sulfate in 1 N H_2SO_4 with an emission quantum yield Φ_{fl} = 0.546.

Single Crystal X-ray Diffraction. Single crystal X-ray diffraction data of **6c**, **7a**, and **10a** were collected at 200, 193, and 150 K, respectively with a Bruker SMART BREEZE diffractometer. The data were solved and refined using SHELXS-2013 and SHELXL-2013, respectively.[31,32] All atoms except for hydrogen were refined with anisotropic displacement parameters and converged for $I > 2(I)$. All calculations were performed with the WinGX-2014 crystallographic software package.[33] Crystallographic data and selective bond lengths of **6c**, **7a**, and **10a** are listed in Tables S1–S7 (Supporting Information). CCDC **1539015 (6c),** CCDC **1539016 (7a)**, and CCDC **1524719 (10a)**.

Results and Discussion

Scheme 1 outlines the synthesis of carbazole–benzimidazole conjugates and corresponding boron dipyrromethene complexes. 1-Formylcarbazole (**4**) was synthesized following the reported procedure.[30] Acid-catalyzed condensation of **4** with 1,2-phenylene diamines afforded the corresponding carbazole–benzimidazole conjugates **6a**, **6b**, and **6c** in good yields. In case of **6a**, the imidazole-NH proton appeared at 13.12 ppm, whereas the carbazole-NH proton appeared at 11.64 ppm. Similar chemical shift values were observed in **6b** (11.26 ppm) and **6c** (11.47 ppm) indicating the existence of the intramolecular N–H•N hydrogen bonding. The unambiguous structural identity of **6c** was confirmed by single crystal X-ray analysis where the intramolecular hydrogen bonding is obvious (Supporting Information). Interestingly, in case of bromo-substituted derivative **9**, the ^{1}H-NMR spectra indicated the existence of the tautomeric form **9a** as shown in Scheme 2.

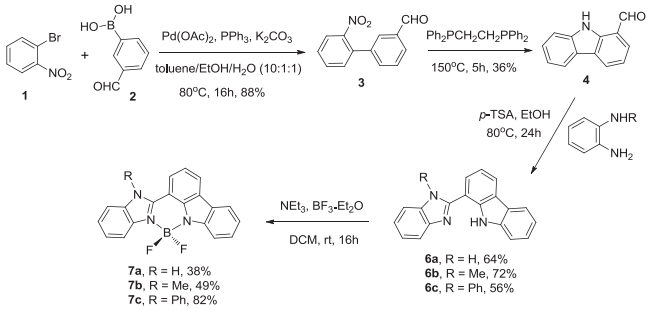

Scheme 1. Synthesis of carbazole–benzimidazole conjugates **6a–6c** and corresponding BODIPYs **7a–7c**. *p*-TSA = *para*-toluenesulfonic acid, DCM = dichloromethane.

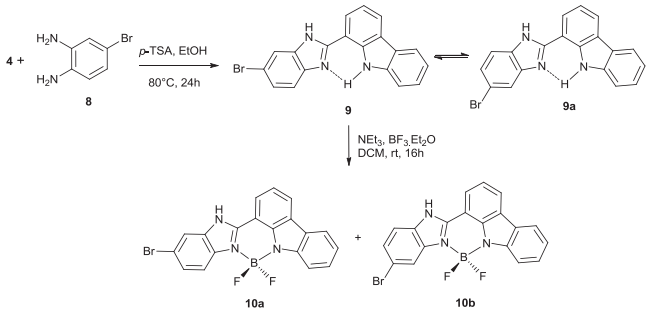

Scheme 2. Synthesis of **9**, **10a,** and **10b.**

Reaction of carbazole–benzimidazole conjugates **6a–6c** with BF_3•OEt_2 in presence of NEt_3 afforded the corresponding BODIPYs **7a–7c** in moderate to good yield. The highest yield of 84% is obtained in case of **6c**. Initially, the formation of the planar boron complexes is expected due to the fact that benzimidazole moiety contains acidic N–H proton. However, the benzimidazole N–H was intact even after the reaction and large downfield shift of benzimidazole N–H signal was observed (14.95 ppm). This observation indicates the coordination of dipyrrin type core with BF_2 unit.

The reaction of the two tautomeric mixture with BF_3•Et_2O resulted in the formation of the two positional isomers **10a** and **10b** as shown in Scheme 2. ^{1}H NMR spectral data analysis of these two isomers revealed slight yet distinct difference in the –NH and –CH signals of the benzimidazole moiety (Supporting Information). The single crystal X-ray analysis of the isomer **10a** unambiguously confirmed the structural identity of the two isomers. The solid state crystal structures of **7a** and **10a** were shown in Figure 1.[34] Briefly, in both cases, the boron atom has a slightly distorted tetrahedral coordination with the two fluorine atoms being perpendicularly oriented with respect to the dipyrrin plane. The B–N bond lengths range from 1.52 to 1.57 Å in **7a** and 1.51 to 1.57 Å for **10a**, indicating that both the complexes possess single B–N bonds. The two B–N distances are virtually identical, implying the expected delocalization of the positive charge. The average B–F bond lengths are 1.39 and 1.38 Å respectively for **7a** and **10a**. Whereas, the N–B–N and F–B–F angles are measured as

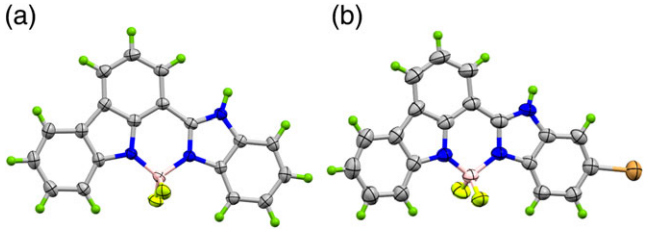

Figure 1. X-ray crystal structures of (a) **7a** and (b) **10a**. Thermal ellipsoids are drawn at 50% probability level. Lattice solvent molecules are removed for clarity.

105.8/107.8° and 106.2/107.9° for **7a** and **10a**, respectively. The carbazole and benzimidazole moieties are found to be co-planar in the BODIPY frameworks in both cases. The crystal packing of both **7a** and **10a** showed aggregation of the BODIPY units with inter planar distance of 3.519 and 3.522 Å respectively (Supporting Information).

All the synthesized BODIPYs displayed similar absorption maxima (λ_{abs}) at ~ 412 nm and vibrational structure ranging from 320 to 280 nm (Figure 2). Fluorescence quantum yields (Φ_{fl}) were obtained by excitation (λ_{ex}) at 314 nm in CH_2Cl_2 with quinine sulfate as the standard (Φ_{fl} = 0.546) (Supporting Information). As summarized in Table 1, the carbazole-based BODIPYs exhibited moderate to high Φ_{fl} values. N–Me substituted BODIPY (**7b**) has slightly higher quantum yield while giving small red-shift to the absorption and blue-shifted emission. Red-shift emission was obtained from N-phenyl (**7c**) derivatives. In both (**10a**, **10b**) derivatives, absorption maxima and emission were red-shifted. Despite of the bromo substituent, compounds **10** still maintained a moderate Φ_{fl} value. Highest Stokes shift ($\Delta\nu_{St}$) was found in compound **7c**, possibly due to the coplanarity of phenyl group with the BODPY framework in excited state. Nevertheless, all compounds showed larger Stokes shifts ranging from 34 to 51 nm compared to the typical BODIPY dyes. A large molar absorption coefficients (ε = 96200 M^{-1} cm^{-1} at 412 nm) was obtained for the compound **7b**. Compound **7c** has 2.5 times higher molar absorptivity than **7a** at 409 nm and the two bromo derivatives (**10a, 10b**) showed relatively lower absorption.

The fluorescence spectra of the synthesized BODIPYs showed close mirror image of the lowest energy absorption band, the typical S^1–S^0 transition. A dramatic absorption coefficient changes were observed in the N-protected benzimidazole **7b** and **7c**. These results indicate that the fine tuning the absorption and emission could be accomplished by introduction of various substituents on the benzimidazole moiety.

The electrochemical redox behavior of the synthesized BODIPYs was studied by cyclic voltammetry. These studies were carried out in CH_2Cl_2 containing 0.1 M TBA•PF_6 with a scan rate of 0.1 V/s at 298 K. The corresponding voltammograms are shown in Figure 3 and the obtained data are summarized in Table 1. **7b**, **7c**, and **10a** showed

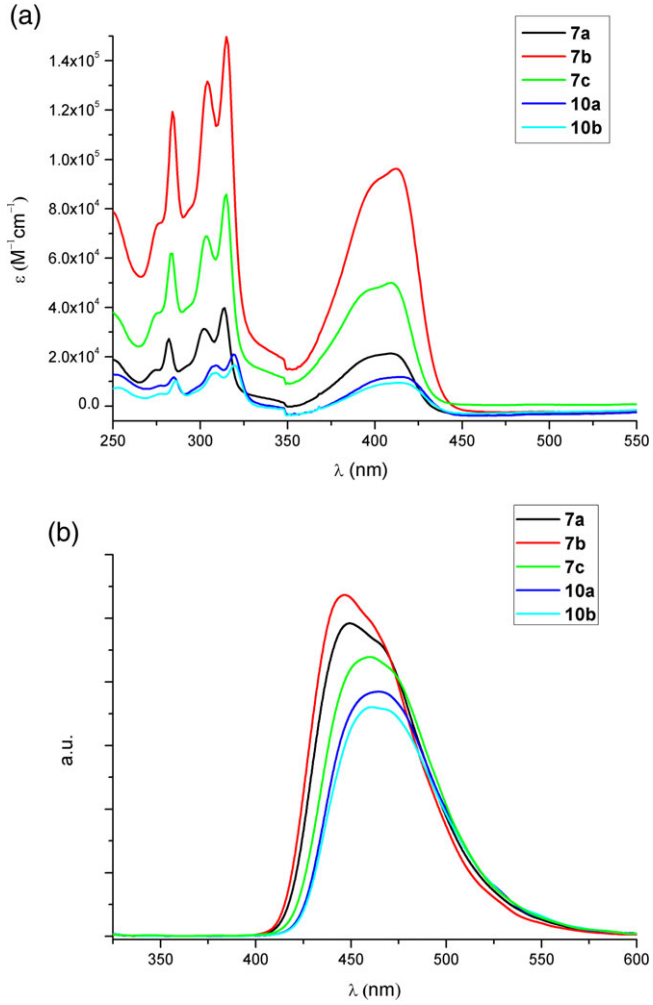

Figure 2. (a) UV–Vis absorption spectra of **7a**, **7b**, **7c**, **10a**, and **10b** in CH_2Cl_2 and (b) fluorescence spectra in CH_2Cl_2 (λ_{ex} = 314 nm).

reversible one electron oxidation and one electron reduction in cyclic voltammogram whereas electrochemical data for **7a** was determined using differential pulse voltammetry (Supporting Information).

The benzimidazole N-substituted analogs **7b** and **7c** showed a marginal cathodic shift of 20–60 mV in oxidation potential as compared to N-unsubstituted **7a**, which is attributed to the electron donating effect of N-methyl and N-phenyl group. The HOMO–LUMO gap (ΔE_{cv}) from the redox potentials correlates fairly well with the HOMO–LUMO gap (ΔE_{opt}) calculated from absorption spectroscopy for these particular BODIPYs as shown in Table 1.

Conclusion

In conclusion we have synthesized novel carbazole–benzimidazole conjugates and corresponding BODIPY dyes. The key synthetic step includes the introduction of substituted benzimidazole at 1-position of carbazole via simple condensation of aldehyde and diamines. UV–Vis,

Table 1. Photophysical properties of BODIPYs as determined from UV–Vis, Fluorescence and cyclic voltammetry in CH_2Cl_2.

Compound	λ_{abs} (ε) [nm($M^{-1}cm^{-1}$)]	λ_{em}^{max} (nm)	$\Delta\nu_{St}$ [nm (cm^{-1})]	Φ_{fl}	E_{ox} (V)	E_{red} (V)	ΔE_{cv} (V)	ΔE_{opt} (V)
7a	409 (21400)	449	40 (2180)	0.60	1.44[a]	−1.76[a]	3.20[a]	3.03
7b	412 (96200)	446	34 (1850)	0.62	1.38	−1.81	3.19	3.01
7c	409 (50000)	460	51 (2710)	0.54	1.42	−1.82	3.24	3.03
10a	416 (11800)	464	48 (2490)	0.47	1.38	−1.80	3.18	2.98
10b	415 (9500)	461	46 (2400)	0.45	n.d.	n.d.	n.d.	2.98

n.d., not determined (due to low solubility); St, Stokes shift.
[a] Data calculated using differential pulse voltammetry.

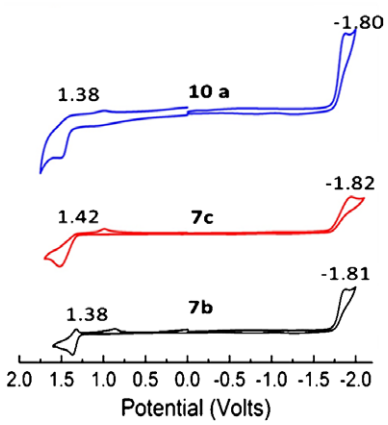

Figure 3. Cyclic voltammograms of **7b** (black), **7c** (red), and **10a** (blue) solvent: CH_2Cl_2, supporting electrolyte: nBu_4NPF_6 (0.10 M), counter electrode: Pt, reference electrode: Ag/Ag^+, working electrode: platinum button (2 mm diameter, scan rate: 01 V/s, rt).

fluorescence, and cyclic voltammometric studies are performed to investigate the photophysical properties. The single crystal X-ray crystallographic analysis further provides the structural insight, particularly in case of the bromo-substituted derivative. π-Extension of the current frameworks for developing red emissive fluorophore is currently under active investigation.

Acknowledgments. Support is acknowledged from the Basic Science Research Program (2015R1A2A1A10052586) funded by the National Research Foundation under the Ministry of Science, ICT & Future Planning of Korea. The central laboratory at Kangwon National University is also acknowledged.

Supporting Information. Additional supporting information is available in the online version of this article.

References

1. A. Loudet, K. Burgess, *Chem. Rev.* **2007**, *107*, 4891.
2. G. Ulrich, R. Ziessel, A. Harriman, *Angew. Chem. Int. Ed.* **2008**, *47*, 1184.
3. H. Kobayashi, M. Ogawa, R. Alford, P. L. Choyke, Y. Urano, *Chem. Rev.* **2010**, *110*, 2620.
4. A. Kamkaew, S. H. Lim, H. B. Lee, L. V. Kiew, L. Y. Chung, K. Burgess, *Chem. Soc. Rev.* **2013**, *42*, 77.
5. N. Boens, V. Leens, W. Dehaen, *Chem. Soc. Rev.* **2012**, *41*, 1130.
6. S. O. Kolemen, A. Bozdemir, Y. Cakmak, G. Barin, E. Erten, M. S. Marszalek, J. H. Yum, S. M. Zakeeruddin, M. K. Nazeeruddin, M. Grätzel, E. U. Akkaya, *Chem. Sci.* **2011**, *2*, 949.
7. L. Wu, K. Burgess, *Chem. Commun.* **2008**, 4933.
8. J. Zhao, K. Xu, W. Yang, Z. Wang, F. Zhong, *Chem. Soc. Rev.* **2015**, *44*, 8904.
9. S. L. Niu, G. Ulrich, R. Ziessel, A. Kiss, P. Y. Renard, A. Romieu, *Org. Lett.* **2009**, *11*, 2049.
10. I. J. Arroyo, R. Hu, G. Merino, B. Z. Tang, E. Pena-Cabrera, *J. Org. Chem.* **2009**, *74*, 5719.
11. A. C. Benniston, G. Copley, *Phys. Chem. Chem. Phys.* **2009**, *11*, 4124.
12. A. B. Nepomnyashchii, A. J. Bard, *Acc. Chem. Res.* **2012**, *45*, 1844.
13. M. Hecht, T. Fischer, P. Dietrich, W. Kraus, A. B. Descalzo, W. E. S. Unger, K. Rurack, *ChemistryOpen* **2013**, *2*, 25.
14. L. Bonardi, G. Ulrich, R. Ziessel, *Org. Lett.* **2008**, *10*, 2183.
15. B. Brizet, C. Bernhard, Y. Volkova, Y. Rousselin, P. D. Harvey, C. Goze, F. Denat, *Org. Biomol. Chem.* **2013**, *11*, 7729.
16. C. Tahtaoui, C. Thomas, F. Rohmer, P. Klotz, G. Duportail, Y. Mely, D. Bonnet, M. Hibert, *J. Org. Chem.* **2007**, *72*, 269.
17. T. Rohand, M. Baruah, W. Qin, N. Boens, W. Dehaen, *Chem. Commun.* **2006**, 266.
18. V. Lakshmi, M. R. Rao, M. Ravikanth, *Org. Biomol. Chem.* **2015**, *13*, 2501.
19. Y. Ni, J. Wu, *Org. Biomol. Chem.* **2014**, *12*, 3774.
20. L. J. Patalag, P. G. Jones, D. B. Werz, *Angew. Chem. Int. Ed.* **2016**, *55*, 13340.
21. H. Lu, J. Mack, Y. Yang, Z. Shen, *Chem. Soc. Rev.* **2014**, *43*, 4778.
22. B. Maji, K. Kumar, M. Kaulage, K. Muniyappa, S. Bhattacharya, *J. Med. Chem.* **2014**, *57*, 6973.
23. Y.-M. Chen, W.-Y. Hung, H.-W. You, A. Chaskar, H.-C. Ting, H.-F. Chen, K.-T. Wong, Y.-H. Liu, *J. Mater. Chem.* **2011**, *21*, 14971.
24. S.-H. Chou, W.-Y. Hung, C.-M. Chen, Q.-Y. Liu, Y.-H. Liu, K.-T. Wong, *RSC Adv.* **2013**, *3*, 13891.
25. C. Maeda, T. Yoneda, N. Aratani, M.-C. Yoon, J. M. Lim, D. Kim, N. Yoshioka, A. Osuka, *Angew. Chem. Int. Ed.* **2011**, *50*, 5691.
26. C. Maeda, T. Todaka, T. Ema, *Org. Lett.* **2015**, *17*, 3090.

27. C. Maeda, T. Todaka, T. Ueda, T. Ema, *Chem. Eur. J.* **2016**, *22*, 7508.
28. M. Más-Montoya, L. Usea, A. E. Ferao, M. F. Montenegro, C. R. de Arellano, A. Tárraga, J. N. Rodríguez-López, D. Curiel, *J. Org. Chem.* **2016**, *81*, 3296.
29. Y. Chen, J. Zhao, H. Guo, L. Xie, *J. Org. Chem.* **2012**, *77*, 2192.
30. H. Peng, X. Chen, Y. Chen, Q. He, Y. Xie, C. Yang, *Tetrahedron* **2011**, *67*, 5725.
31. G. M. Sheldrick, *SHELXS-2013 - A Program for Automatic Solution of Crystal Structures*, University of Goettingen, Goettingen, **2013**.
32. G. M. Sheldrick, *SHELXL-2013 - A Program for Crystal Structure Refinement*, University of Goettingen, Goettingen, **2013**.
33. L. J. Farrugia, *J. Appl. Cryst.* **2012**, *45*, 849.
34. CCDC numbers: compound **6c** (**1539015**), compound **7a** (**1539016**), and compound **10a** (**1524719**). Crystallographic data for **6c**: empirical formula: $C_{25}H_{13}N_3$; formula weight: 359.42; triclinic; space group *P*-1, a = 7.7905(8), b = 10.1199(10), c = 11.5115(11) Å; α = 79.595(2), β = 77.311(2), γ = 80.513(2); V = 863.39(15) Å^3; Z = 2; λ *(Å)* = 0.71073; *T (K)* = 150.0(2); ρ_{calcd} (g · cm^{-3}) = 1.379; *R (F)* = 0.0414; $R_w(F_o^2)$ = 0.1078. Crystallographic data for **7a**: empirical formula: $C_{19}H_{12}BF_2N_3$, CH_3OH; formula weight: 363.17; monoclinic; space group $P2_1/c$, a = 9.7161(2), b = 21.6267(6), c = 8.1052(2) Å; α = 90, β = 97.709(2), γ = 90; V = 1687.73(7) Å^3; Z = 4; λ *(Å)* = 0.71073; *T (K)* = 193.0(2); ρ_{calcd} (g · cm^{-3}) = 1.429; *R(F)* = 0.0413; $R_w(F_o^2)$ = 0.1043. Crystallographic data for **10a**: empirical formula: $C_9H_{11}BN_3F_2Br$, CH_3OH; formula weight: 442.07; monoclinic; space group $P2_1/n$, a = 9.5062(2), b = 10.0486 (2), c = 19.3612(3) Å; α = 90, β = 94.5180(10), γ = 90; V = 1843.71(6) Å^3; Z = 4; λ *(Å)* = 0.71073; *T (K)* = 200.0 (2); ρ_{calcd} (g · cm^{-3}) = 1.593; *R(F)* = 0.0433; $R_w(F_o^2)$ 0.1075.

